Journal Pre-proof

A dual macrophage polarizer conjugate for synergistic melanoma therapy

Marwa A. Sallam, C. Wyatt Shields, Supriya Prakash, Jayoung Kim, Daniel C. Pan, Samir Mitragotri

Please cite this article as: M.A. Sallam, C. Wyatt Shields, S. Prakash, et al., A dual macrophage polarizer conjugate for synergistic melanoma therapy, *Journal of Controlled Release* (2021), https://doi.org/10.1016/j.jconrel.2021.05.033

This is a PDF file of an article that has undergone enhancements after acceptance, such as the addition of a cover page and metadata, and formatting for readability, but it is not yet the definitive version of record. This version will undergo additional copyediting, typesetting and review before it is published in its final form, but we are providing this version to give early visibility of the article. Please note that, during the production process, errors may be discovered which could affect the content, and all legal disclaimers that apply to the journal pertain.

A dual macrophage polarizer conjugate for synergistic melanoma therapy

Marwa A. Sallam[1,2], C. Wyatt Shields IV [1,3], Supriya Prakash[1], Jayoung Kim[1], Daniel C. Pan[1], Samir Mitragotri[1*]

[1] John A. Paulson School of Engineering and Applied Sciences, Harvard University, Cambridge, MA 02138, USA; Wyss Institute of Biologically Inspired Engineering, Harvard University, Boston, MA 02115, USA

[2] Department of Industrial pharmacy, Faculty of pharmacy, Alexandria University, Egypt.

[3] present address: Department of Chemical and Biological Engineering, University of Colorado Boulder, Boulder, CO 80309, USA

* Corresponding author: mitragotri@seas.harvard.edu

Abstract

Tumor associated macrophages (TAMs) play a paradoxical role in the fate of aggressive tumors like melanoma. Immune modulation of TAMs from the tumor-permissive M2 phenotype to antitumoral M1 phenotype is an emerging attractive approach in melanoma therapy. Resiquimod is a TLR7/8 agonist that shifts the polarization of macrophages towards M1 phenotype. Bexarotene (BEX) is a retinoid that induce the expression of phagocytic receptors in macrophages besides its ability to downregulate the M2 polarization. However, the clinical use of both agents is hindered by poor pharmacokinetic properties. Here, for the first time we repurposed BEX based on its immunomodulatory properties and combined it with RES by designing hyaluronic acid (HA) conjugates of both drugs that act synergistically as a dual macrophage polarizer to promote the M1 phenotype and suppress the M2 phenotype. This combination enhanced the macrophage secretion of proinflammatory cytokines (IL-6 and TNF-α), while suppressing the production of tumor promoting cytokine CCL22. It enhanced the macrophage phagocytic ability and showed superior inhibitory effects against B16F10 cells. *In vivo* studies on a mouse melanoma model confirmed the superiority of the dual conjugate

compared to the single HA-drug conjugates in suppressing the tumor growth. Immunoprofiling of the excised tumors revealed a significant increase in the M1/M2 ratio of TAMs in mice treated with the dual conjugate. Our intravenously injectable HA conjugate of RES and BEX provides a promising immunotherapeutic combination strategy for resetting the M1/M2 ratio, supporting the tumoricidal activity of TAMs for effective melanoma treatment.

Key words

Polymer conjugates, antitumor, macrophage, polarization, melanoma.

1. Introduction

Melanoma is one of the most aggressive forms of skin cancer, causing a large majority of skin related deaths worldwide [1]. It is treated by surgery, radiation and chemotherapy. Although surgery is the standard treatment for skin cancers including melanoma, it is ineffective against metastatic tumors [2]. Moreover, treatments often end in recurrence. Hence, immunotherapy aimed at modulating the tumor microenvironment is gaining significant attention since it has the advantage of taming the body's immune system to tackle metastasis and develop a memory response against recurrence. Most immunotherapies focus on the administration of an immunomodulatory agent, sometimes in addition to a checkpoint inhibitor. This approach, despite being effective, still faces some limitations [3].

Tumor-infiltrating leukocytes (TILs) are currently the focus of immunoediting strategies aimed at the treatment of melanoma and other forms of cancer [4]. Tumor-associated macrophages (TAMs), are one of the most abundant TILs in solid tumors. TAMs display a wide range of phenotypes that are capable of performing different functions [5, 6]. However, this phenotypic diversity is often simplified into an ostensible M1/M2 dichotomy, with the anti-inflammatory (tumor-permissive, M2) phenotype on one side and proinflammatory (antitumoral, M1) phenotype on the other side [7-9]. In most solid tumors, TAMs tend to polarize towards an M2 rather than the M1 phenotype, thereby assisting tumor development by inducing immune suppression and angiogenesis while suppressing the activity of other effector cells including CD8$^+$ and CD4$^+$ T-cells [10-12]. There have been substantial efforts either to deplete the M2 TAMs or to repolarize them towards an M1 phenotype [13]. The approaches to deplete the TAMs have shown promising outcomes in delaying tumor progression in experimental animals

and have moved to clinical evaluation [14-18]. However, considerable interest is being directed towards the second approach exploring the use of small molecule receptor inhibitors for reprogramming TAMs by abolishing their tumor supportive functions and promoting their antitumor immune functions [19-21]. It has been reported that the use of CSF1R small molecule inhibitors altered the polarization of TAMs and resulted in controlling the progression of glioblastoma [22]. In a recent study, the combined use of the same molecule with Src homology region 2 (SH2) domain-phosphatases SHP-2 inhibitor successfully inhibited melanoma growth by TAMs repolarization pathway [23]. Despite the progress in this area, there is still a critical need for the development of effective therapeutic approaches to re-educate the TAMs with higher potency. Interferon gamma (IFN-γ) is a known M1 polarizer that is reported to suppress tumor growth, however its off-target side effects hinder its clinical use.

Among the various classes of immune-modulatory agents, toll-like receptors (TLR) agonists are powerful immune modulators stimulating the innate immune system, activating antigen presenting cells (APCs) and polarizing TAMs. Resiquimod (RES) is an imidazoquinoline TLR7/8 agonist that binds to endosomal membrane receptors [24]. It is more potent than imiquimod (a TLR7 agonist approved for topical treatment of skin malignancies) [25]. It promotes the polarization of TAMs toward an M1 phenotype [26]. Despite its reported effectiveness in suppressing the growth of several types of cancer, currently it is only available in the market as a topical gel. However, topical application is not effective against deep cutaneous tumors like melanoma due to poor absorption. Moreover, systemic administration is hindered by poor bioavailability [27]. It has been reported that the incorporation of small molecule TLR agonist in cyclodextrin nanoparticles alters the tumor immune microenvironment, which was not

observed with systemic administration of the free drug [26]. Recently, encapsulation of RES into polymeric micelles has proven effective in chemo-insensitive non-small cell lung cancer. However, the combination of anti-PD-1 with RES micelles did not provide any benefit over RES micelles alone, suggesting lack of synergy between them [24]. Accordingly, other effective synergistic combinations for melanoma immunotherapy still need to be explored.

A phase II clinical trial in melanoma patients demonstrated an augmented immunotherapeutic response when ATRA was administered with ipilimumab [28]. ATRA is a retinoid reported to enhance antitumor immunity by promoting differentiation of immature myeloid cells into macrophages, inhibiting the immunosuppressive effect of myeloid-derived suppressor cells on CD8$^+$ T-cell-mediated immunity [29]. This finding illustrates the potential benefit of implementing retinoids in combination with immunotherapeutic agents to combat melanoma.

Herein, we selected bexarotene (BEX), a retinoid X receptor (RXR) agonist that has proven effective against different types of cancer and is approved by the FDA for treating cutaneous T-cell lymphoma. We repurposed BEX based on its immunomodulatory properties represented by its ability to diminish myeloid-derived suppressor cells [30], to downregulate the M2 polarization of macrophages [31] and to enhance their phagocytic ability. BEX has been recently reported to induce the expression of phagocytic receptors in macrophages and enhance erythrophagocytosis in brain hematomas [32]. However, this property has not been harnessed in combination cancer immunotherapy. The studies on efficacy of BEX against several types of

tumors have focused on its direct effect on cancer cells but its poor solubility and poor bioavailability limit its clinical use [33].

In this work we explore the feasibility of combining BEX (as M2 down regulator) and RES (as M1 up regulator) and studied the efficacy in a mouse melanoma model. By delivering both agents simultaneously to the site of action, we aim to synergistically modulate TAM polarization by suppressing M2 phenotype, and at the same time, promote M1 phenotype, thereby favorably altering the M1/M2 ratio and enhancing the TAM phagocytic capabilities.

A key challenge in administering drug combination is that both molecules have different pharmacokinetic profiles that can hinder their effective simultaneous delivery to the target site [23, 34]. To overcome this challenge, we conjugated both agents to the same polymer. We leveraged hyaluronic acid (HA) for the codelivery of RES and BEX given its characteristic property to target CD44, an integral cellular membrane glycoprotein expressed on macrophages [35, 36]. Additionally, HA is biocompatible, biodegradable and plays an important role in cancer therapy as being able to provide target-specific delivery and reducing systemic toxicity. Herein, we report a hyaluronic acid conjugate of RES and BEX to HA. We evaluated the effect of the conjugates on bone marrow-derived macrophages (BMDMs) with respect to their viability, activity, phenotype and phagocytic ability. The inhibitory effect of the conjugates against the B16F10 melanoma cell line was investigated. The therapeutic efficacy of the conjugates was evaluated in a subcutaneous mouse melanoma model.

2. Experimental section

2.1. Materials

The materials used in this study are described in Supporting Information (SI).

2.2. Synthesis of HA-BEX and HA-RES and HA-RES-BEX dual conjugate

For the synthesis of HA-BEX, 50 mg of 50 kDa MW HA (0.13 mmol of HA acid units) were dissolved in 3 mL DMF under stirring and slight heating (50˚C). 12 mg of BEX (0.034 mmol) were dissolved in 200 μL DMSO followed by the addition of 13.5 mg EDC (0.07 mmol) and 4 mg (0.033 mmol) of DMAP dissolved in DMSO. The mixture was stirred for 1 hr then was added to the HA solution. The reaction was allowed to proceed for 48 hr. The product was purified using Sephadex G-25 PD-10 desalting columns equilibrated in MilliQ water. The product was further purified by dialysis at 4˚C for 24 hr and was lyophilized (SP Scientific Freezemobile) for further characterization.

For the synthesis of HA-RES, 50 mg of HA (0.13 mmol HA units) was dissolved in 5 mL MES buffer at pH 6.5, 25 mg EDC and 15 mg NHS were added. The mixture was stirred for 45 min at room temperature. Activated HA was separated from the reaction products by centrifugal filters (MWCO, 3 kDa) with repeated washing with PBS. 20 mg of RES (0.065 mmol) dissolved in 500 μL DMSO were added to the activated HA. The reaction mixture was stirred for 24 hr and was then purified by dialysis for 24 hr (Slide-A-Lyzer™ 3.5K MWCO) followed by lyophilization of the product.

For the synthesis of the dual conjugate, 50 of HA-RES conjugate was dissolved in 3 mL DMF. The carboxylic group of BEX (12 mg) was activated by adding 13.5 mg EDC and 4 mg DMAP and stirring for 1 hr at room temperature then was added to the HA-RES solution and

stirred at 50°C for 48 hr. The product was precipitated in ethanol/PBS mixture. The unconjugated BEX was measured in the supernatant by HPLC (see Methods in the SI).

The conjugates were characterized by ^{1}H NMR. Drug loading of HA-BEX was determined by UV-Vis measurements performed using plate reader (SpectraMax i3x) at λ_{max} of 260 nm. For HA-RES, drug content was measured by quantifying the fluorescence of RES at an excitation and emission wavelengths of 260 and 360 nm, respectively. Chemical structures of HA conjugates were verified with ^{1}H NMR. Conjugates were dissolved into D_2O at 5–7 mg/mL and analyzed with a Varian VNMRS (600 MHz) spectrometer. Data was processed using MestReNova software (Bruker GmbH, Karlsruhe, Germany).

The physical structure of the HA-BEX, HA-RES and dual conjugate (HA-RES-BEX) was observed using transmission electron microscopy (Hitachi 7800). The size and zeta potential of the conjugates was determined by dynamic light scattering (Malvern Zetasizer NanoZS instrument; details in the SI).

2.3. Synthesis of fluorescent HA-RES and HA-RES-BEX

HA was labeled with Alexa Flour 488 or Alexa Flour 647, as previously described.[37] Fluorescent HA-RES was prepared following the same procedure used for the synthesis of HA-RES using HA labeled with Alexa Flour 488, while the fluorescent dual HA-RES-BEX conjugate were prepared with Alexa Flour 488 for cellular uptake and with Alexa Flour 647 for the biodistribution study.

2.4. BMDM isolation and culture

Femurs and tibias were harvested from C57BL/6 mice, the epiphyses of each bone were cut, and the bones were flushed with PBS using a syringe with a 31G needle into a 50 mL collection tube. The procedure was performed under sterile conditions. The solution was passed through a 40 μm cell strainer then centrifuged at 350xG for 10 min at 4°C. Cells were resuspended in Bambanker (Lymphotec, Inc.) and stored in cryovials at –80°C until further use [38].

To culture BMDMs, the frozen bone marrow was thawed, added to 5 mL of BMM⁻ (i.e., DMEM F12, with 5% FBS, 1% mL of Pen/Strep, and 2.5% of 200 mM GlutaMAX) at 4°C and centrifuged at 350xG for 5 min. The supernatant was aspirated, and the pellets were resuspended in BMM⁺ (i.e., BMM⁻ with 20 ng/mL macrophage colony-stimulating factor, M-CSF), and cultured in non-tissue culture (non-TC) treated T175 flasks containing in 25 mL BMM⁺ media under standard conditions. On the third day, additional BMM⁺ was added to the flasks. After 6 days, the media was removed, cells were washed with HBSS and harvested from the flask using Accumax^TM. The cell suspension was added to an equal volume of BMM⁻, centrifuged and the supernatant was aspirated. The obtained BMDMs were resuspended in BMM⁺ and then used for the subsequent studies.

2.5. Effect on viability of BMDMs and cytokine secretion

BMDMs were seeded in 96-well plates at a density of $5x10^3$ cells/well and placed in humidified incubator maintained at 37°C and 5% CO_2 (Thermo Scientific, USA) for 24 hr. The media was then aspirated and replaced with increasing concentration of BEX, RES, HA-BEX, HA-RES and their combinations at predetermined ratios. The plates were kept under standard conditions for 48

hr, after which point the supernatant was collected in microcentrifuge tubes and replaced with 10% alamarBlue (AB) solution in BMM^- and incubated for 3 hr in the dark at 37°C. Finally, cellular viability was assessed by reading the florescence of the solution from each well at $\lambda_{ex} =$ 560 nm and $\lambda_{em} = 590$ nm (SpectraMax i3x). Baseline fluorescence levels from wells without cells were subtracted from each data point. The collected supernatant was analyzed for cytokines production including IL-6, TNF-α and CCL22 using ELISA assay after appropriate dilutions following the manufacturer protocols.

2.6. Internalization of the conjugates by BMDMs

The internalization of fluorescently labeled conjugates was assessed by confocal microscopy and by flow cytometry. BMDMs ($5x10^3$ cells) were plated in individual chambers of Nunc™ Lab-Tek™ II Chamber Slide™ System (Thermo Scientific) and allowed to adhere overnight. The media was then aspirated and replaced with 200 μL of fluorescently labeled conjugate, followed by incubation for 4 hr at 37°C. The treatments in the wells were completely aspirated and cells were washed twice with PBS. Hoechst 33342 (10 μL of 0.5 mM solution) and the lysosomal marker LysoTracker Red (10 μL of 100 nM solution) were added and incubated 20 min before washing with PBS and fixing with 4% paraformaldehyde. The fixed cells were imaged using confocal microscopy (Upright Zeiss LSM 710 NLO ready, Germany). Alexa Flour 488 and Alexa Flour 647 were imaged using excitation/emissions of 638 / 756 nm and 493 / 517 nm, respectively. For flow cytometry analysis, $5x10^4$ BMDMs were plated in 12-well plates as previously described to allow for adhesion. The plates were then aspirated, and 1 mL of fresh media was added to each well. 200 μL of the fluorescent dual conjugate was added to each well incubated for 4 hr at 37°C. After the predetermined time points were reached, media in the wells

was completely aspirated. The cells were washed twice with HBSS then were detached from plate using 1 mL Accumax, added to 1 mL BMM$^-$ centrifuged and resuspended in flow cytometry buffer before being analyzed by flow cytometry (BD LSR Analyser II, CA, USA)

2.7. *Quantitative uptake of HA-conjugates by BMDMs*

BMDMs were seeded in sterile 6-well plates at a density of 10^6 cell/well overnight. On the next day, the media was aspirated and replaced with 50 μM of each of free RES, equivalent amount of HA-RES, HA-RES-BEX-Alexa 488 in fresh BMM$^+$ media. To study the effect of HA-mediated uptake, cells were treated with free HA in an amount equal to that used in the conjugates for a period of 2 hr, followed by the addition of the conjugates. After 4 hr, the supernatants were aspirated, the cells were washed twice with 2 mL HBSS and the cells were treated with 2 mL of 0.5% solution of Triton X- 100 for 3 hr for lysing. The lysate was centrifuged, and the supernatant was analyzed for fluorescence on a SpectraMax i3x plate reader for the quantification of RES. The uptake of HA-RES-BEX-Alexa 488 was measured by flow cytometry. The experiment was performed in triplicate for each treatment.

2.8. *In vitro activity of conjugates against B16F10-Luc cells in a co-culture with BMDMs*

B16F10-Luc cells were cultured in DMEM media supplemented with 10% FBS, 1% Pen Strep and 0.1% puromycin under standard conditions. The cells were seeded in 96-well plates at a density of $5x10^3$/well and allowed to adhere overnight. For establishment for a co-culture, B16F10-Luc cells were co-cultured with BMDMs at a ratio of 1:10 ($5x10^3$ B16F10 cells to $5x10^4$ BMDMs per well). The next day, the media was aspirated and replaced with increasing concentration of the free drugs, their combination and the HA-conjugates with equivalent drug

concentrations. The cells were incubated with the different treatments for 48 hr after which the supernatant was aspirated and replaced with 200 μL of 0.5% Xenolight-D-luciferin potassium salt solution in complete DMEM. Finally, cellular viability was assessed by reading the luminescence of the solution from each well after 10 min using BioTek plate reader with the untreated cells used as controls.

2.9. Phenotyping in vitro cultures of BMDMs

BMDMs were seeded in non-TC treated 12-well plates at a density of 2.5×10^4 cells/well. On the next day the media was aspirated, and the cells were treated with predetermined concentration of each of free RES, free BEX, their individual HA conjugates, combined conjugates at different ratios and dual conjugate. After 48 hr, the supernatants were aspirated and replaced with 1 mL Accumax after washing with HBSS. Plates were incubated for 15 min at 37°C and 5% CO_2, followed by vigorous agitation to dislodge the BMDMs. The suspension from each well was added to 1 mL BMM$^-$ and centrifuged at 350xG for 5 min at 4°C. The cell pellets were resuspended in 1 mL of cell staining buffer (1% FBS in PBS) and centrifuged again. The cell pellets were resuspended in 100 μL of staining buffer containing 1 μL Fc block (anti-mouse CD16/CD32) and were incubated for 20 min at 4°C. For surface staining, samples were centrifuged and resuspended in an antibody mixture of anti-MHCII and anti-VEGF, according to manufacturer specifications dark at 4°C (see SI (Table S1) for details on the fluorescence of each antibody). After 30 min, cells were washed with 1 mL staining buffer, centrifuged, resuspended in 300 μL of staining buffer before analysis. For intracellular staining, samples were fixed and permeabilized following instructions from the manufacturer (BD Biosciences). Cells were resuspended in 100 μL of an antibody solution composed of anti-iNOS, anti HIF-1α and anti-

CD206 in Perm/Wash^{TM} Buffer according to manufacturer specifications (see SI (Table S1) for details on the fluorescence of each antibody). Cells were kept at 25°C in the dark for 30 min, after which they were diluted with 1 mL of Perm/Wash^{TM} Buffer, centrifuged and resuspended in 300 µL of stain buffer for analysis. Up to 10,000 events were collected for each sample. Data were analyzed using FCS Express 7 Software (De Novo Software).

2.10. In vitro phagocytosis assay

BMDMs were stained by VivoTrack 680 (PerkinElmer) according to manufacturer protocol and plated into non-TC treated 12-well plates (2.5×10^5 cells/well) overnight. Cells were incubated with the different treatments including HA-RES, HA-BEX and their combination (HA-RES/HA-BEX) each at concentration equivalent to 25 µM of each drug for 48 hr. B16F10 melanoma cells were labeled with CellTrace Violet, following the manufacturer protocol and were incubated (10^5 cells/well) with the stained treated BMDMs at a ratio of 1:2.5. After 4 hr, the supernatant was aspirated, the cells were dislodged as previously described for the BMDMs and then suspended in cell staining buffer for analysis by flow cytometry. Percentage of phagocytosis was determined by the percentage of violet positive cells within red stained BMDM cell gate.

2.11. In vivo biodistribution studies

B16F10-Luc melanoma cells (10^6) were implanted subcutaneously in the fat pad of 6–8 weeks old C57BL/6 mice (weighing 20 g, Charles River Laboratories). All experiments were performed according to the approved protocols by the Institutional Animal Care and Use Committee (IACUC) of Harvard University. Fourteen days after inoculation, mice were administered 100 µL of 20 mg/mL Alexa 647-labeled HA-RES-BEX dual conjugate via tail vein injection. Mice were euthanized at 4 and 8 hr post-injection. Surgically resected organs were thoroughly washed

with PBS and imaged using IVIS filter set (excitation 640 nm and emission 680 nm). All images were taken using a PerkinElmer IVIS Spectrum CT In Vivo Imaging System (IVIS). The organs were then weighed, homogenized in PBS using a high shear homogenizer (IKA T 10 Basic ULTRA-TURRAX, NC, USA) and homogenates were treated with equal volumes of methanol, centrifuged at 20,000xG for 15 min and the supernatants were analyzed for fluorescence intensity using a calibration curve of the fluorescent HA conjugate in the organ homogenate.

2.12. Efficacy study on mouse melanoma model

B16F10-Luc (10^6) were implanted subcutaneously in the fat pad of 6–8 weeks old C57BL/6 mice (weighing 20 g, Charles River Laboratories). At day 8 after tumor inoculation, the treatment was started. Mice were divided into four groups (n = 5), receiving HA-RES, HA-BEX, the dual conjugate (HA-RES-BEX) and a control group (saline). The mice were given a dose equivalent to 5 mg/kg body weight on days 8, 11, 14 and 19. The mice were imaged using *in vivo* imaging (PerkinElmer IVIS Spectrum, MA, USA) on days 7, 10, 13, 18 and 21. For this, mice were injected intraperitoneally with 150 µL of XenoLight-D-luciferin (30 mg/mL) in PBS. Fifteen minutes after the injection, mice were imaged using IVIS. The tumor volumes and body weights were monitored every other day. Tumor volumes were calculated using the formula, $L \times B^2/2$, where the L is longest diameter and B is the shortest diameter as measured using a digital caliper. Two days after the last injection, mice were euthanized via CO_2 inhalation. Tumors were harvested immediately following sacrifice and processed for analysis.

2.13. Flowcytometric analysis of excised tumor samples

Harvested tumors were weighed, then each tumor was cut into small pieces and enzymatically degraded using Miltenyi mouse tumor dissociation kit with a gentle MACS dissociator, according to manufacturer protocol. The resultant suspension was passed through a 70 μm to remove debris, flushed with DMEM and centrifuged. The pellet was resuspended in ACK red cell lysis buffer. After 5 min, the cells were centrifuged and resuspended in staining buffer for cells counting. The cell suspension was divided into different groups each of 10^6 cells per animal and were stained using the similar procedure to that used in the polarization study. All steps were performed in 100 μL FACS buffer. Cells were incubated with 1% anti-mouse CD16/32 antibody (BioLegend) for 20 min on ice in the dark to block Fc receptors. Cells were then stained with antibodies for surface and intracellular markers. Different panels of antibody mixtures were made from CD45, F4/80, CD11b, CD11c, CD86, iNOS, CD206, MHCII, VEGF, CD3 and CD8 (the fluorescence and supplier of each antibody are listed in Table S1) and Live/Dead Cell Staining Kit (Thermo Scientific). After staining, cells were washed twice and analyzed using flow cytometry (BD LSRII). Non stained cells were used as negative control. Compensation beads, each stained with one antibody were used for single color controls. Data were analyzed using FCS Express 7 Software.

2.14. Statistical analysis

The data were represented as mean ± SD using GraphPad (Prism 8.0). For determination of statistical significance, multiple t-tests or one-way ANOVA with Dunnett's multiple comparison tests were used, as applicable. Significance was determined at the following cutoff points ($p < 0.05 = *$, $p < 0.01 = **$, $p < 0.001 = ***$ and $p < 0.0001 = ****$).

3. Results

3.1. Synthesis and characterization of HA-RES and HA-BEX conjugates

A carbodiimide coupling reaction procedure was adopted for the direct attachment of RES and BEX to HA backbone via amide and ester bond, respectively **(Figure 1A).** The conjugates were characterized using a number of techniques to confirm identity and drug loading. ^{1}H NMR spectroscopy data indicated the conjugation of RES to HA **(Figure 1B).** HA-RES showed a characteristic peak at 1.88 ppm characteristic of the acetamido moiety (CH_3-g) of HA, aliphatic protons of RES at 1.1–1.2 ppm and aromatic peaks at 7.28-8.26 ppm confirming that RES was successfully conjugated with a molar content of 4.5–5.0 mol.%, indicated by peak integration **(Figure S1A).** HA-RES drug content was further quantified by fluorescence measurement at an excitation and emission wavelength 260 nm and 390 nm, respectively. For HA-BEX, ^{1}H NMR data showed the characteristic peak for HA at 1.88 ppm, peaks for aliphatic protons of BEX at 0.93–1.15 ppm and peaks for aromatic protons at 7.67 and 7.87, revealing 6.7 mol.% content, as determined by peak integration **(Figure S1B).** This was further confirmed by UV spectroscopy. UV-Vis analysis confirmed drug loading of HA-BEX where the conjugate preserved the characteristic maximum absorbance of the parent drugs (λ = 260 nm). We optimized the synthetic procedure to adjust the loading of both drugs in the dual conjugate ensuring the consistency of the yield **(Figure S1C).** Drug loading of about 4.5 and 5.5 wt.% could be achieved for RES and BEX, respectively in the dual HA-RES-BEX conjugate. The conjugates formed aqueous dispersions without any visible aggregates.

TEM micrographs illustrated that the conjugates formed self-assembled spherical structures **(Figure 1C)** with hydrodynamic diameters of 98.7 ± 13.6, 119.4 ± 11.5 and 192 ± 21.2

nm and zeta potential values of –43.6, –44.7 and –35.7 mV for HA-RES, HA-BEX and the HA-RES -BEX dual conjugate, respectively. These data provided an indication of the satisfactory properties of dual conjugate for systemic delivery (i.e., hydrodynamic radius and zeta potential are important aspects for efficient delivery to the tumor).
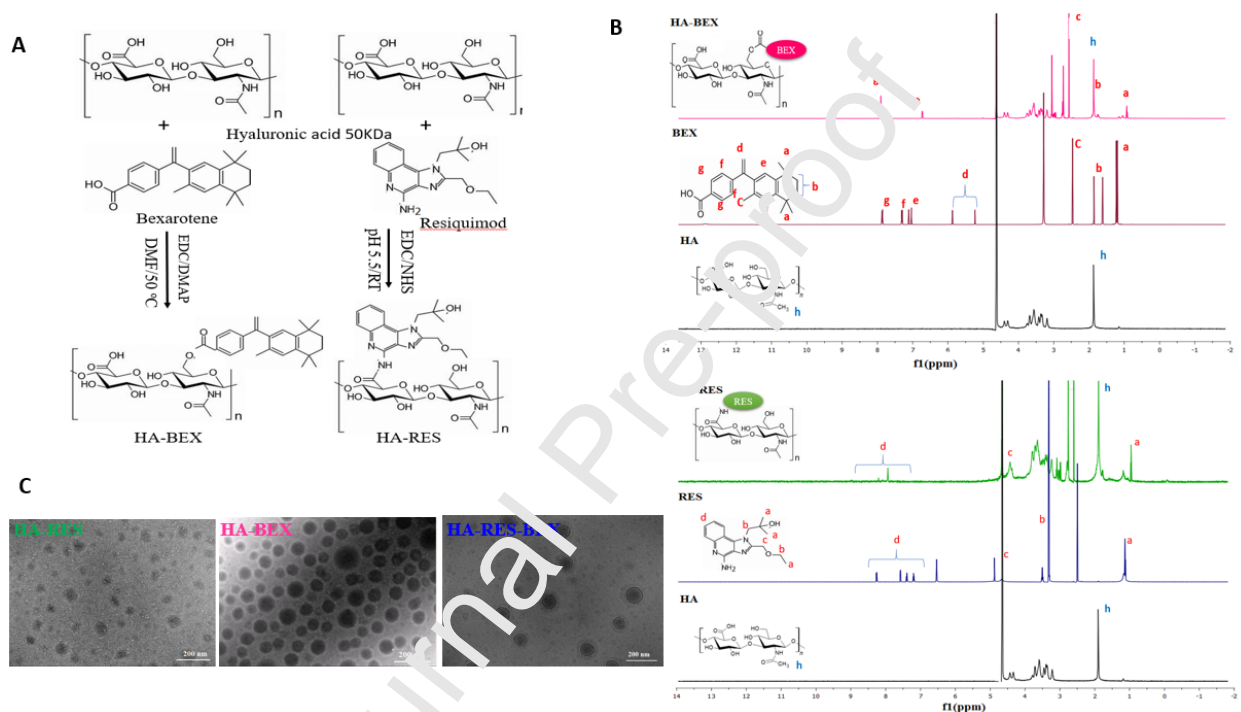

Figure 1. Synthesis and characterization of HA conjugates. (A) Schematic illustration of the synthetic procedure for HA-BEX and HA-RES. (B) ^{1}H NMR data of HA-BEX (top) and HA-RES (bottom) showing the assignment of BEX and RES peaks, respectively. (C) TEM micrograph of self-assembled HA-BEX, HA-RES and HA-RES-BEX dual conjugate spherical structures.

3.2. Biological activity of HA-BEX and HA-RES

3.2.1. Effect on BMBM viability and cytokines secretion

Immune cells such as macrophages and dendritic cells are responsible for initiating immune responses and represent key targets for immunostimulatory drugs [39]. HA-RES conjugates were well-tolerated by BMDMs after a 48 hr exposure. Neither free RES nor its HA-conjugate displayed a cytotoxic effect on BMDM viability. Instead, an increase in cell viability was observed at all concentrations tested (**Figure 2A**). Enhanced cell viability of BMDMs and bone marrow-derived dendritic cells in the presence of RES has been previously reported [24, 39].

The conjugation of TLR agonists to different molecules has been reported to alter their activity and receptor specificity [40]. Therefore, we sought to test whether the conjugate still retained the immunostimulatory effects of the parent molecule. We assessed the proinflammatory cytokines in the supernatant of BMDM cultures after 48 hr of exposure to RES and HA-RES. The secretion of proinflammatory cytokines such as tumor necrosis factor alfa (TNF-α) and interleukin-6 (IL-6) serve as quantitative indicators for TLR7 activation of BMDMs [24]. HA-RES induced the secretion of TNF-α and IL-6. The induction of proinflammatory cytokines was similar for HA-RES and the equivalent amount of free RES, indicating that conjugation of RES to HA did not affect its immunological activity (**Figure 2B and 2C**). Moreover, the levels of TNF-α and IL-6 detected where much higher than those produced by cells treated with 20 ng/mL IFN-γ (202 ±18 and 130 ± 8.8 pg/mL for TNF-α and IL-6, respectively). Also, since RES is a synthetic ligand of the endosomal receptor TLR7, delivery to the endosome of phagocytic cells is essential for its immunological activity [41]. We incubated BMDMs with fluorescently labeled

HA-RES for 4 hr and observed endosomal localization of the conjugate, confirming that the cargo was delivered to its intended intracellular target **(Figure 2D).**

We also tested the effect of BEX and its HA conjugate on the viability of BMDMs at various concentrations (0.39–50 μM). We found that both the free BEX and its HA conjugate did not alter the viability of the BMDMs at any tested concentration up to 25 μM, after which point further increase in the concentration of drug caused a significant decrease in cellular viability **(Figure 2E).** An important mechanism underlying the activity of BEX against cancer is its ability to reduce the production of CCL22 from TAMs, as reported in a recent clinical study [31]. CCL22 is a C-C chemokine receptor type 4 (CCR4) ligand that attracts CCR4$^+$ T-cells, including regulatory T-cells (Tregs), promoting melanoma growth [42]. CCL22 vaccination is reported to suppress melanoma growth by decreasing Treg recruitment to the tumor. An assessment of the effect of HA-BEX on the production of CCL22 from BMDMs indicated that the conjugate retained the ability of BEX to reduce the secretion of CCL22 levels in the supernatant of BMDM cultures **(Figure 2F).**

Interestingly, co-administration of HA-RES with HA-BEX to BMDMs did not show a negative effect on cellular viability at all concentrations tested. Even HA-BEX at concentration of 50 μM, which showed a reduction in BMDM viability, did not show any inhibition of BMDMs when combined with HA-RES (i.e., the combination of HA-RES with HA-BEX even at the lowest concentration of RES 0.03 μM enhanced BMDM viability; **Figure S2**).

We also measured the level of cytokines in the supernatant of BMDM cultures after 48 hr treatment with HA-RES, HA-BEX and their combinations. There was an increase in the

production of IL-6 and TNF-α (up to 30- and 75- fold respectively compared to untreated cells), while there was a significant reduction in the production of CCL22 secreted by macrophages polarized toward M2 phenotypes (i.e., by 20 ng/mL IL-4) prior to adding the conjugates **(Figure 2G).** These results indicate that the combination of HA-RES and HA-BEX may act together as a promising combination by promoting upregulating proinflammatory cytokines, such as IL-6 and TNF-α on one side, while inhibiting the production of CCL22 on the other side, which together with TLR8-mediated suppression of Tregs [43] could be a promising opportunity for cancer immunotherapy.
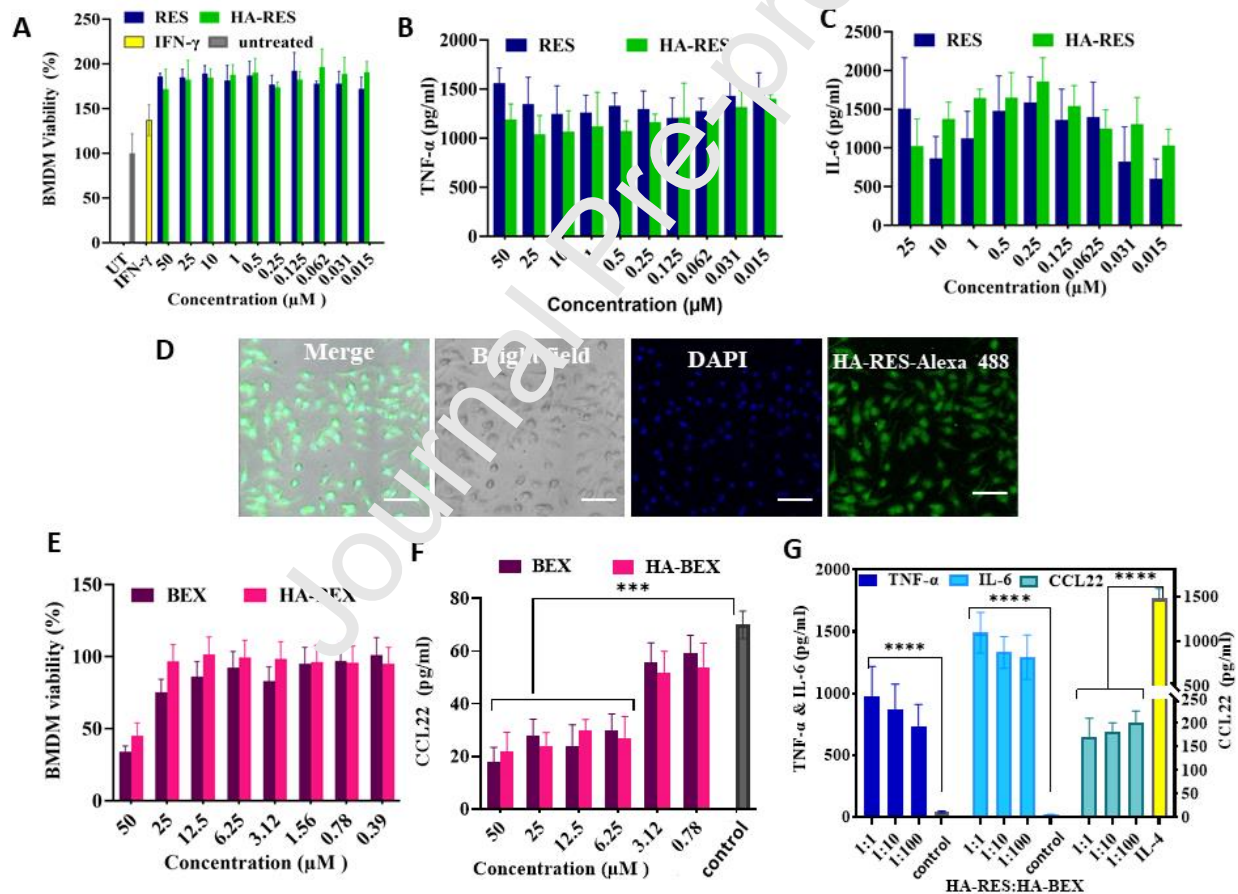

Figure 2. Effect of HA-RES, HA-BEX and their combination on BMDM viability and production of proinflammatory cytokines (n = 3). (A) RES and HA-RES enhances the viability

of BMDMs. (B) Production of TNF-α and (C) IL-6 from BMDM after 48 hr treatment with RES and HA-RES. (D) Confocal laser scanning micrographs (CLSM) showing the internalization of Alexa Fluor 488-labeled HA-RES by BMDM after 4 hr incubation, scale bar 50 μm. (E) Effect of BEX and HA-BEX at different concentrations on the viability of BMDMs, and (F) the production of CCL22 in the supernatant of BMDM cultures. (G) Effect of combining HA-RES and HA-BEX at selected ratios on the production of TNF-α, IL-6 and CCL22.

3.2.2. Dendritic cell maturation

We further tested the effect of the conjugates on activating dendritic cells (DCs), which have the most potent antigen presentation capability among APCs [39] We evaluated the expression of CD11c, MHCII and CD86 as maturation markers for DCs, given their important role for effective T-cell priming required for adaptive immunity [44-46]. DCs exposed to RES, BEX, HA-RES and HA-BEX expressed higher levels of the maturation markers MHCII and CD86 compared to the untreated cells (Fig. S3). This confirmed that HA-RES maintains its immunological activity and highlights for the first time the stimulatory effect of HA-BEX on DCs. Interestingly, the cells treated with a combination of HA-RES and HA-BEX showed a significant increase in the expression of MHCII ($p < 0.05$) and highly significant increase in the expression of CD86 ($p < 0.0001$) compared to the cells treated with a single conjugate, indicating the synergistic immune stimulatory activity of this combination.

3.2.3. BMDM polarization

Upon verifying the lack of toxicity of conjugates to BMDMs, we further elucidated the effect of HA-RES and HA-BEX and their combination on macrophage polarization. BMDMs were treated

with different concentrations of RES and HA-RES for 48 hr. The expression of several markers associated with M1 and M2 phenotypes was evaluated and normalized to untreated BMDMs **(Figure 3A).** We evaluated the relative expression of M1 biomarkers, including iNOS, which is involved in the production of nitric oxide (NO) that serves as a potent tumoricidal agent [47] and HIF-1α, which is reported to be a promotor of M1 polarization.[48, 49] We also evaluated the expression of CD206 and vascular endothelial growth factor (VEGF) as representative M2 markers[50].

Cells treated with either free RES or HA-RES demonstrated a 2.0 to 2.2-fold increase in the expression of iNOS compared to untreated cells. The expression of CD206 was reduced to 0.7-fold compared to untreated cells. We compared the level of marker expression to that induced by IFN-γ (a potent M1 polarizer) [50]. Interestingly, the fold change in iNOS expression induced by the drug conjugate was higher than that induced by IFN-γ, which only showed a 1.3-fold increase compared to untreated cells **(Figure 3A).** This further confirmed that conjugating RES to HA did not affect its ability to polarize BMDMs. The effect was not dependent upon the concentrations tested. Treatment of BMDMs with different concentrations of BEX or HA-BEX did not show a significant change in the expression of iNOS compared to untreated cells; however, it reduced the expression of CD206, which was 0.5 to 0.6-fold of that expressed by untreated cells, representing a1.66-2 fold reduction in the expression. **(Figure 3B).** HIF-1α is a metabolic regulator that participates in the M1 polarization of macrophages [48, 49]. BMDMs treated with either HA-RES, HA-BEX or free drugs at different concentrations showed a 2.0 to 3.0-fold increase in the relative expression of HIF-1α compared to the untreated cells. However, the fold change was less than that induced by IFN-γ, which showed a 5.5-fold increase in the expression of HIF-1α compared to untreated cells.

Interestingly, BMDMs treated with combinations of HA-RES and HA-BEX showed up to a 4.3- fold increase in the expression of iNOS relative to untreated cells, which was significantly higher than that induced by HA-RES or HA-BEX alone. In addition, the combination demonstrated a 6.0 to 7.0-fold increase in the expression of HIF-1α compared to untreated cells. This increase was significantly higher than that induced by the individual conjugates. Moreover, the expression of CD206 on cells treated with the combination of conjugates was reduced to 0.35-fold compared to untreated cells, demonstrating a significant reduction compared to that induced by each individual conjugate **(Figure 3C).** This indicated that the drug combination can act synergistically as potent dual macrophage polarizer by simultaneously promoting M1 phenotypes and suppressing M2 phenotypes.

Many reports show that the polarization state of macrophages is reflected in their morphology [26]. We observed the morphology of BMDMs after different treatments. Following treatment with HA-RES, cell morphology shifted from elongated structures with projections observed in untreated BMDMs to round, and flattened structures, characteristic of M1 activated macrophages. BMDMs treated with a HA-BEX/HA-RES showed mostly a round morphology **(Figure 3D).**
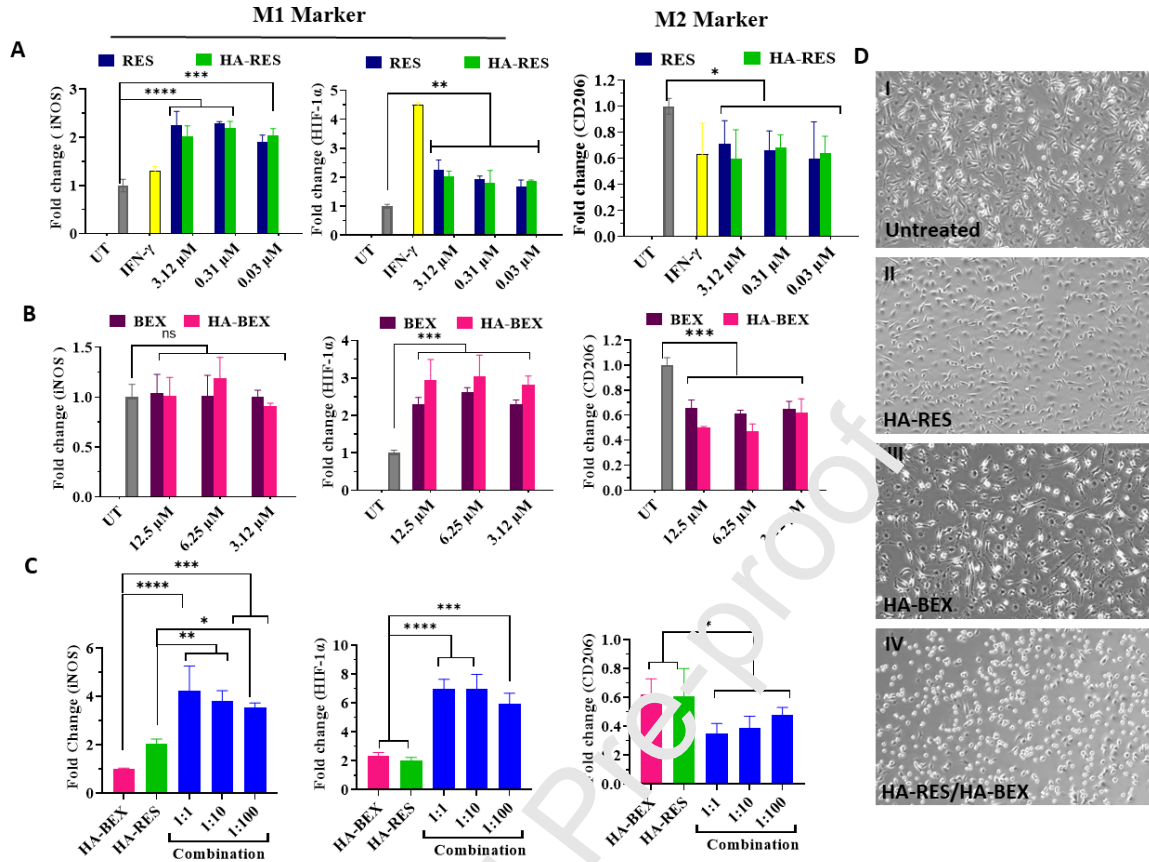
Figure 3. Phenotypic evaluation of BMDMs in response to free drug and drug conjugates in vitro. (A) BMDMs were treated with different concentration of RES and HA-RES, (B) BEX and HA-BEX and (C) combinations of HA-RES and HA-BEX at selected ratios. Bar graphs indicate the fold change in the median expression of selected M1 and M2 biomarkers relative to their expression in untreated BMDMs (n = 5; ns, non-significant; *$p < 0.05$; **$p < 0.01$; ***$p < 0.001$; ****$p < 0.0001$). (D) Cell morphology of BMDMs after treatment with HA-RES, HA-BEX and combination conjugates showing: (I) elongated structures with projections observed in untreated BMDMs, shifting to (II) round, and flattened structures when treated with HA-RES, (III) a lower proportion of elongated cells treated with HA-BEX and (IV) a higher proportion of round cells observed upon treatment with a combination HA-BEX/HA-RES.

3.2.4. Cytotoxicity study against melanoma cells

We studied the ability of conjugates to inhibit the growth B16F10-Luc (luciferase-expressing melanoma cells) cultured alone and in co-culture with BMDMs. RES had a negligible cytotoxic effect on melanoma cells. Its effect on B16F10-Luc cells was significantly enhanced in the presence of macrophages **(Figure 4A).** In other words, RES or its HA-conjugate did not exhibit direct inhibitory effects against B16F10 cells. The reduced cell viability of the melanoma cells in the co-culture with the BMDMs is likely attributed to its immunomodulatory effect on BMDMs. This observation is consistent with previous studies, where RES did not exhibit any cytotoxic activity against lung adenocarcinoma cells (344SQ) despite its *in vivo* efficacy [24]. BEX had an IC50 of 25.2 μM on B16F10. The inhibitory effect of BEX (at low concentrations) was improved in the presence of BMDMs **(Figure 4B).**

The combination of free BEX and free RES did not result in a measurable enhancement of cytotoxicity. Interestingly, the combined conjugates were more potent in inhibiting the growth of melanoma cells. While the IC50 of BEX on B16F10 cells is 25.2 μM, adding free RES at equimolar concentration to BEX did not add to this effect. However, combining both conjugates at the same concentration resulted in 100% inhibition of melanoma cells. The combination of the HA-BEX / HA-RES conjugates caused a 2.2-fold reduction in IC50 of BEX (11.22 μM).

At a concentration of 12.5 μM, the free drug combination caused 13.6% inhibition of cell viability, while the combined conjugates caused 62.7% inhibition of cell viability. Perhaps more interesting was the significant reduction in B16F10 viability observed at all of tested concentrations of the combined conjugates in the co-culture with BMDMs **(Figure 4C).**

3.2.5. Cellular uptake

We studied the quantitative uptake of the free RES and its HA conjugate by BMDMs. To study

the effect of HA-mediated uptake, cells were incubated with free HA in an amount equal to that

used in the conjugates to occupy the HA receptors before adding the conjugates. The uptake of

HA-RES was 4-fold higher than free RES. However, upon pretreatment with HA, the uptake of

HA-RES diminished (24-fold decrease). This suggests that the uptake is mediated through HA

receptors (CD44) expressed on the BMDMs **(Figure 4D).** Accordingly, HA conjugates can allow

for the use of a 4-fold lower dose of RES while achieving the same effective amount of uptake

by macrophages. This highlights the privilege of the HA conjugates over the free drug in

reducing the dose administered, thus likely reducing the side effects associated with higher drug

doses.

Delivering the conjugate bearing both drugs into the cellular compartment ensures that

they will act simultaneously. To confirm this, we synthesized fluorescently labeled dual loaded

conjugate (HA-BEX-RES-Alexa Fluor 488) and studied its uptake by BMDMs. Flow cytometry

analysis of the uptake revealed that cells treated with HA prior to the conjugate exhibited 13.4-

fold reduction in the fluorescence intensity compared to those treated directly by the conjugate

confirming the data obtained from the previous quantitative uptake experiment **(Figure 4E).**

3.2.6. Phagocytosis study

The polarization of macrophages toward M1 phenotypes is reported to enhance their phagocytic

and tumor clearing capabilities [23, 51]. Accordingly, we performed a phagocytosis assay to

understand the mechanism underlying the enhanced inhibitory effect of the combined conjugates

compared to the single conjugates in co-cultures with BMDMs **(Figure 4G).** We observed that BMDMs treated with a combination of HA-RES and HA-BEX had a significantly higher phagocytic index compared to BMDMs treated with the individual conjugates or untreated BMDMs **(Figure 4H).** These results indicated that superior activity of the combined conjugates manifested by the higher inhibition of the B16F10 cells co-cultured with BMDMs could be attributed to the synergistic activity of both HA-RES and HA-BEX in promoting M1 shifting enhancing the phagocytic ability of BMDMs, resulting in phagocytosis of the cancer cells rather than direct toxic effect of the drugs on them.
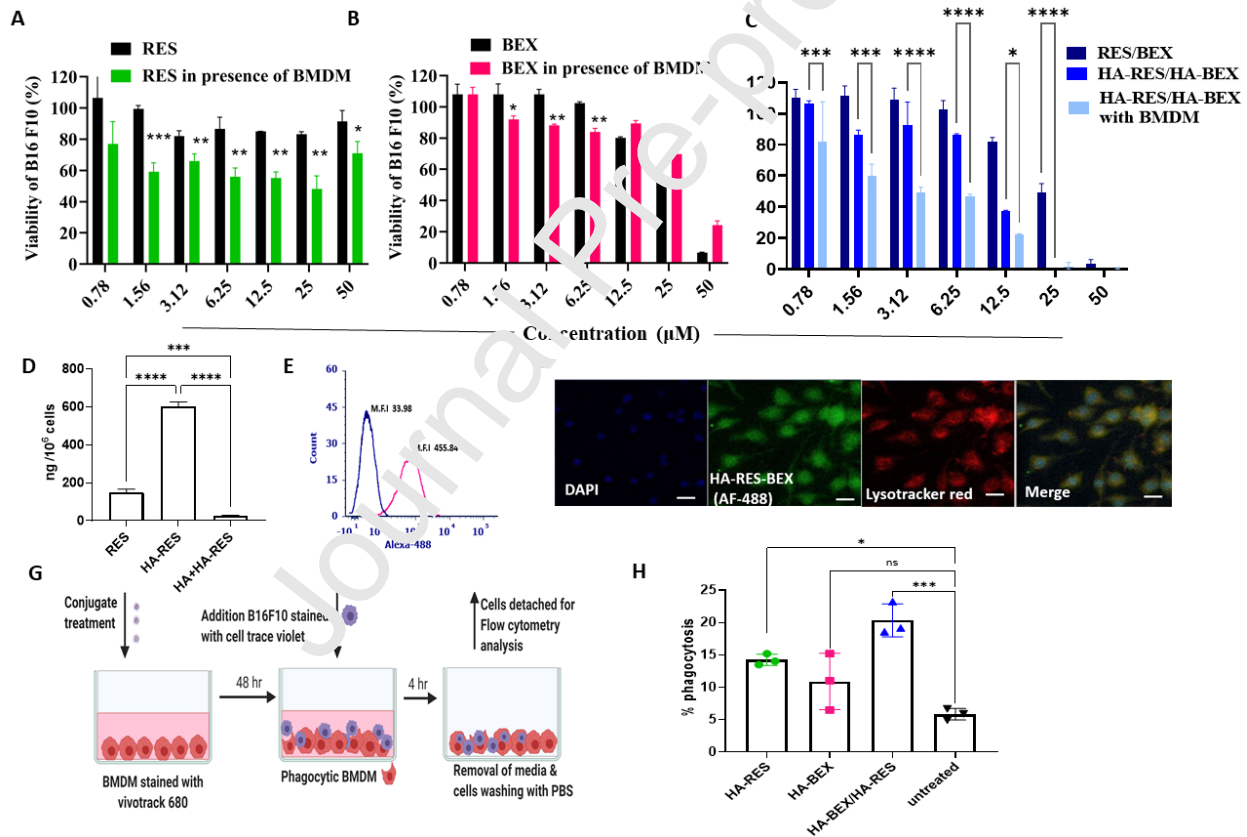

Figure 4. In vitro efficacy against melanoma cells and a mechanistic study of the conjugates superiority. (A, B, C) Effect of HA-RES, HA-BEX and their combination on the viability of B16F10-Luc melanoma cells co-cultured with BMDMs (n = 3). (D) Quantitative uptake of the

HA-RES by BMDMs. (E) Flow cytometry histogram showing the uptake of HA-BEX-RES-Alexa Fluor 488 by BMDMs with and without pretreatment of the cells with an equivalent amount of HA. Blue line: uptake of the florescent conjugate applied 2 hr after pretreatment of the cells with an equivalent amount of HA. Pink line: uptake of the conjugate without HA pretreatment (higher florescence intensity). (F) Confocal microscopy images showing the localization of the dual conjugate within the lysosomal compartment of the BMDMs, scale bar 20 µm. (G) Schematic representation of the phagocytosis study. BMDMs stained by VivoTrack 680 and incubated with the different treatments for 48 hr. B16F10 melanoma cells labeled with CellTrace Violet were incubated with BMDMs at a ratio of 1:2.5. Percentage of phagocytosis was determined by flow cytometry by quantifying the percentage of violet-positive cells within the red-stained BMDM cell gate. (H) Percentage of BMDMs that were phagocytic in a coculture B16F10. Bars represent mean ± standard deviation (SD) (n = 3).

3.3. In vivo assessment of conjugates

We sought to validate our *in vitro* results by studying the efficacy of the drug conjugates on a B16F10 melanoma model *in vivo*. Many studies reported that the use of a dual conjugate was more effective *in vivo* than the physical mixture of single drug conjugates[52-54]. When we tested the effect of the dual conjugate on the BMDM polarization and tested its cytotoxicity against B10F16 cells, there was not a significant difference between the dual conjugate and the mixture of the individual conjugates **(Figure S4).** However, attaching both drugs to the same polymer backbone would have the advantage of allowing both drugs to circulate together overcoming the differences in their pharmacokinetics and allowing them to accumulate at the tumor simultaneously. Accordingly, we proceeded to the *in vivo* study using the dual conjugate.

We first assessed the biodistribution of the dual conjugate in tumor bearing mice after intravenous injection **(Figure S5).** The amount detected in the tumor after 4 and 8 hr was 43.53 ± 9.37 and 51.65 ± 7.15 µg/g of tissue, which corresponds to approximately 2.17 and 2.51 µg of the conjugated drugs, respectively. A large amount of the conjugate was found to localize in the reticuloendothelial organs, including the liver, lungs and the spleen, which is an important target for generating systemic immunity (e.g., in developing cancer vaccines) [55].

Therapeutic efficacy of conjugates was assessed in mice burdened with B16F10 tumors **(Figure 5A).** We monitored the progression of the tumors each day. A significant reduction in tumor size was observed in the group treated with the combination conjugate compared to groups treated with the single conjugates and the control (saline) group **(Figure 5B, C, D).** Changes in the body weights fell within the acceptable limits, indicating that the treatments were not generally toxic **(Figure 5E).** We measured serum cytokine levels (TNF-α and IL-6) in tumor-bearing mice 48 hr after the last injection to screen for potential systemic toxicity, and we found no significant difference in the levels of TNF-α and IL-6 in serum between groups **(Figure S6).** This finding agrees with previous studies reporting that proinflammatory cytokines show normal levels 24 hr after the administration of TLR agonists at doses commensurate with those used in this study [24].

Ex vivo analysis of tumor-associated immune cells was performed to assess the impact of conjugates on tumor microenvironment **(Figure 5F, G, H).** Profiling of tumor-associated immune cells showed that groups receiving HA-RES and dual conjugate exhibited an increase in the percentage of iNOS-expressing cells (CD45$^+$/F4/80$^+$/iNOS$^+$) compared to the control untreated group. The effect was highly significant for the dual conjugate treated group (P =

0.0002). Further, a reduction in the percentage of cells expressing CD206 (M2) was observed for all the treatment groups, which was highly significant for the dual conjugate treated group. Overall, all treatment groups exhibited a significant increase in the M1/M2 intracellular markers ratio with the group treated with the dual conjugate eliciting the highest increase (p=0.0003 compared to p = 0.021 and p = 0.0022 for HA-BEX and HA-RES respectively) **(Figure 5H).**

Interestingly, all the treatment groups showed a reduction in VEGF expression which was significant (P=0.006) for the HA-RES treated group and highly significant (P=0.0008) for the dual conjugate treated group **(Figure S7A),** although *in vitro* tests indicated there was not a significant change in the expression of VEGF after BMDMs treated with HA-RES or HA-BEX or their combination. VEGF is known to be overexpressed in TAMs, acting as a source of angiogenic cytokines that promote tumor vascularization.[50] Moreover, a significant increase in MHCII-expressing TAMs (CD45$^+$/F4/80$^+$/MHCII$^+$) was observed in groups treated with HA-RES and the dual conjugate **(Figure S7B)** despite the fact that the *in vitro* studies showed no significant difference in the relative expression of MHCII between BMDMs treated with the conjugates and untreated BMDMs.

The differences observed in the expression of some markers between the *in vitro* and *in vivo* study can be attributed to the fact that the *in vitro* models of macrophage polarization might not be fully representative of the immunosuppressive TAM phenotype which can only be accurately achieved within the *in vivo* tumor microenvironment being endowed with a cocktail of immunosuppressive cytokines as well as the interaction between various APCs *in vivo* [26]. Analysis of DC population (CD45+/CD11b+/CD11c+) revealed that tumors resected from the

group treated with the dual conjugate exhibited significantly higher levels of the maturation marker CD86 compared to the control group **(Figure S7C).** CD86 is involved in the priming and activation of T cells upon interaction with DCs that constitutes the first crucial signal for T cell priming. In looking at the T- cell population (CD45+/CD3+/CD8+), for HA-BEX treated group the percent of T-Cells was 1.7- fold lower than that the of dual conjugate group (p=0.031). For HA-RES treated group, the percent of T- cells was higher than that of the control group (P=0.046) but it was 1.4-fold less than that of dual conjugate treated group that showed the highest percent of T- cells among all the groups and it demonstrated a highly significant increase compared to the control group (P= 0.001) **(Fig S7D).**

In agreement with our *in vitro* results, the increase in the M1/M2 ratio, the activation of DC, and subsequent increase in the CD8+ cytotoxic T-cell tumor infiltration reveals to be the underlying mechanism for the enhanced antitumor activity of the dual conjugate. Our results indicate that the combination conjugates of BEX and RES effectively repolarize TAMs toward an antitumor phenotype *in vivo* in melanoma bearing mice, validating the *in vitro* study with BMDMs.
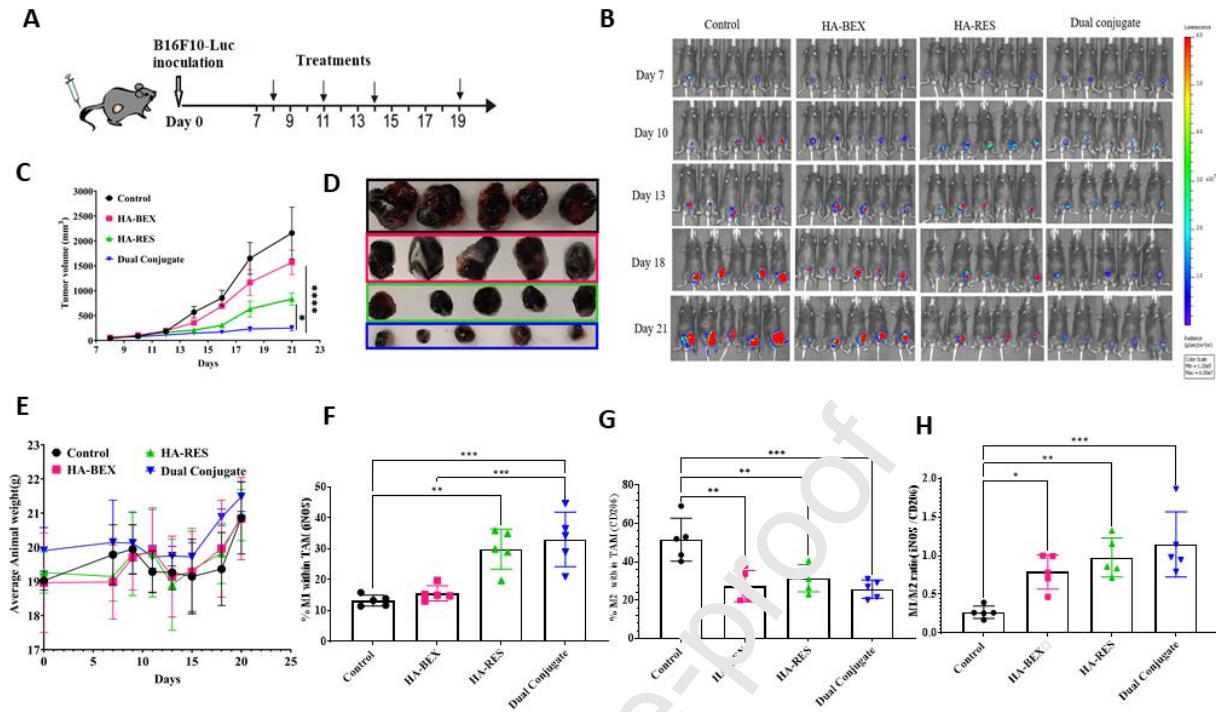
Figure 5. In vivo efficacy of HA-RES, HA-BEX and dual conjugate in a B16F10-Luc mouse model. (A) Schematic chart of the treatment schedule. (B) Bioluminescence images of subcutaneous melanoma at different time points after tumor inoculation. (C) Tumor growth profiles and (D) corresponding images of melanoma tumors excised from the mice at the time of study termination. (E) Weights of mice were monitored to reflect the general well-being of the animals. No mouse lost more than 15% body weight in the period of the study (n = 5). (F-H) Phenotypic evaluation of TAMs for mice given HA-BEX, HA-RES, or the dual conjugate compared to control untreated mice. Each data point represents one mouse. Bars represent the mean ± SD. (F) Percentage of iNOS-expressing TAMs (CD45$^+$/F4/80$^+$/iNOS$^+$) (M1 marker). (G) Percentage of CD206-expressing TAMs (CD45$^+$/F4/80$^+$/CD206$^+$) (M2 marker). (H) M1/M2 ratio of TAMs determined from (F) and (G).

4. Discussion

The results presented here demonstrate therapeutic designs that use combination immunomodulatory agents for improved antitumor efficacy. We introduce a rational strategy for the co-delivery of two immunomodulatory agents (RES and BEX) by conjugating them to HA to act synergistically together as a dual macrophage polarizer and synergistic stimulant for DCs. The conjugation of RES and BEX to HA provides an injectable form of two poorly soluble drugs and allows delivery of both drugs to the tumor site at the same time, which cannot be achieved by the free drugs due to their different pharmacokinetics and biodistribution. Hence, polymer conjugation of these drugs was performed. We first evaluated the invitro activity of either HA-RES and HA-BEX on BMDM, DCs and B16F10 cells. After we verified that the individual conjugates retain the activity of the parent drug molecules, we studied the effect of combining them to test any synergistic effect. Since this is the first study that combines RES and BEX we used the physical mixture of both drug conjugates (HA-RES/HA-BEX) for the *in vitro* studies which allowed us to combine them at different ratios understand the synergy between the two drugs and to identify optimal combinations. The combination of HA-BEX and HA-RES synergistically stimulated the DCs and shifted BMDMs toward M1 phenotypes, enhancing their phagocytic ability and showed enhanced activity against B16F10 cells. Accordingly, we synthesized the dual conjugate at a molar ratio 1:1 of both drugs. This dual nanoconjugate was successfully taken up by the macrophages without affecting their viability. The enhanced uptake is mediated by HA receptors. The dual conjugate showed similar invitro effect to the combined conjugates on BMDM and B16F10 cells. While both the combination of the individual conjugates and the dual conjugate exhibit similar invitro efficacy, only the latter can ensure simultaneous exposure to tumor cells and can provide a means to capture the *in vitro* cellular efficacy *in vivo*, as well[56, 57]. Therefore, we proceeded to the *in vivo* studies to compare the

effect of the dual conjugate with each of the individual drug conjugates. *In vivo* studies in an aggressive mouse melanoma model revealed the ability of such an injectable combination conjugate to reach the tumor and exhibit a significant suppression of tumor growth rate compared to the individual conjugates. Analysis of the tumor-associated immune cells revealed a significant enhancement of the M1/M2 ratio validating our hypothesis. Moreover, the dual conjugate enhanced DCs maturation and increased the percentage of tumor infiltrating CD8+T-Cells. A schematic representation of the proposed mechanism of our conjugate is illustrated in Figure 6. While not investigated in this study, the ability of our treatment to skew the TAM M1/M2 ratio towards an M1 phenotype and consequently restoring the immune function of tumor infiltrating CD8+ T-cells might be effective against tumors that are refractory to immunotherapy due to deficient tumor-penetrating T lymphocytes ("cold tumors"). Since we introduce this combination for the first time, further studies to investigate if this combination can improve the outcome of T-cell directed treatments as anti-PD-1 worth consideration. Another important aspect of this combination conjugate is the possible development of immunological memory that can suppress tumor recurrence. However, realization of such a system requires further investigation.
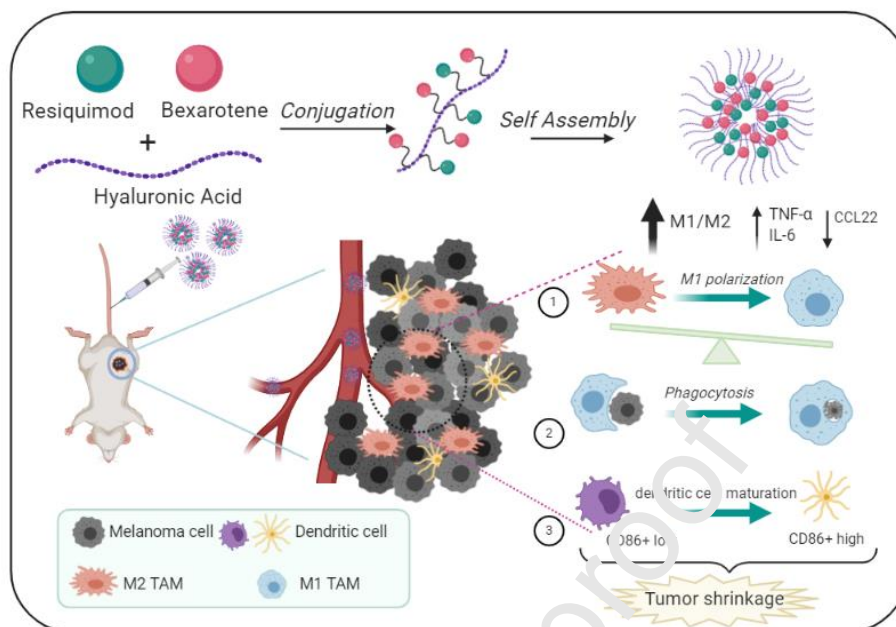
Figure 6. Schematic illustration of the design and mechanism of action of the dual conjugate for melanoma treatment.

Despite the absence of any toxicity signs on the experimental mice, a limitation of the clinical translation of this combination conjugate might be the potential side effects arising from systemic administration. The dose of 5 mg/kg of both drugs that was used in this study was based on previous reports that such dose (3-6 mg/Kg) for RES is well tolerated in mice, while for BEX this is much lower than the tolerated dose reported in literature (50-150 mg/kg). Given the therapeutic efficacy observed with the dosing decided in this study, it may be interesting to investigate the efficacy at lower doses as well. Future studies could also be directed towards local intratumoral injection of this combination conjugate and evaluating its therapeutic efficacy to minimize any side effects that may potentially arise from systemic administration.

To our knowledge, this is the first study introducing a polymer conjugate combination of small molecules that act by altering the TAM phenotypes on both sides (i.e., by upregulating M1-associated factors and downregulating M2-associated factors simultaneously). Previous studies on polymer conjugates for cancer therapy has focused on combining chemotherapeutic drugs that act by synergistic direct effect on cancer cells.[58]

5. Conclusion

We designed a polymer conjugate of two immunomodulatory drugs to dually regulate the polarization of macrophages for cancer treatment. The simultaneous delivery of both agents resulted in enhanced antitumor efficacy against aggressive mouse melanoma model. Our approach of modulating the TAM phenotype with a polymer combination conjugate of small molecules opens the door for future investigations on other types of solid tumors. The biodistribution of the conjugate and its ability to accumulate in the RES organs and intestines suggests its potential application to target tumors in those organs. Conjugating both drugs to HA provides the advantage of overcoming the solubility and pharmacokinetic limitations of the drugs alone, allowing a single administration of both agents simultaneously, potentially eliminating the need for alternating dosing schedules that is commonly practiced in combination immunotherapies.

with flow cytometry, Z. Zhao of Harvard University for helpful discussions and help on the

animal model. We acknowledge using https://www.biorender.com in creating Figure 6.

Author statement

M.S. and S.M. designed the research. M.S., C.W.S, S.P., J.K., D.P. performed the experiments,

M.S., C.W.S. and S.M. analyzed the data. M.S. and S.M. wrote the paper with revisions from all

authors. S.M. conceived the project.

Conflict of interest

S.M. and M.S. are inventors on patent applications related to polymer drug conjugates.

References

[1] V. Mundra, W. Li, R.I. Mahato, Nanoparticle-mediated drug delivery for treating melanoma, Nanomedicine (Lond), 10 (2015) 2613-2633.
[2] R. Wilken, M. Criscito, A.C. Pavlick, M.L. Stevenson, J.A. Carucci, Current Research in Melanoma and Aggressive Nonmelanoma Skin Cancer, Facial Plast Surg, 36 (2020) 200-210.
[3] L. Ambrosi, S. Khan, R.D. Carvajal, J. Yang, Novel Targets for the Treatment of Melanoma, Curr Oncol Rep, 21 (2019) 97.
[4] R.D. Schreiber, L.J. Old, M.J. Smyth, Cancer immunoediting: integrating immunity's roles in cancer suppression and promotion, Science, 331 (2011) 1565-1570.
[5] W. He, N. Kapate, C.W.t. Shields, S. Mitragotri, Drug delivery to macrophages: A review of targeting drugs and drug carriers to macrophages for inflammatory diseases, Adv Drug Deliv Rev, (2019).
[6] F.O. Martinez, S. Gordon, The M1 and M2 paradigm of macrophage activation: time for reassessment, F1000Prime Rep, 6 (2014) 13.
[7] J. Zhou, Z. Tang, S. Gao, C. Li, Y. Feng, X. Zhou, Tumor-Associated Macrophages: Recent Insights and Therapies, Front Oncol, 10 (2020) 188.
[8] V. Bronte, P.J. Murray, Understanding local macrophage phenotypes in disease: modulating macrophage function to treat cancer, Nat Med, 21 (2015) 117-119.
[9] T.A. Wynn, A. Chawla, J.W. Pollard, Macrophage biology in development, homeostasis and disease, Nature, 496 (2013) 445-455.
[10] M. De Palma, C.E. Lewis, Macrophage regulation of tumor responses to anticancer therapies, Cancer Cell, 23 (2013) 277-286.
[11] A. Mantovani, P. Allavena, The interaction of anticancer therapies with tumor-associated macrophages, J Exp Med, 212 (2015) 435-445.
[12] Y. Komohara, Y. Fujiwara, K. Ohnishi, M. Takeya, Tumor-associated macrophages: Potential therapeutic targets for anti-cancer therapy, Adv Drug Deliv Rev, 99 (2016) 180-185.
[13] A. Mantovani, F. Marchesi, A. Malesci, L. Laghi, P. Allavena, Tumour-associated macrophages as treatment targets in oncology, Nat Rev Clin Oncol, 14 (2017) 399-416.
[14] B. Ruffell, L.M. Coussens, Macrophages and therapeutic resistance in cancer, Cancer Cell, 27 (2015) 462-472.
[15] P. Sharma, J.P. Allison, The future of immune checkpoint therapy, Science, 348 (2015) 56-61.

[16] Y. Wang, Y.X. Lin, S.L. Qiao, H.W. An, Y. Ma, Z.Y. Qiao, R.P. Rajapaksha, H. Wang, Polymeric nanoparticles promote macrophage reversal from M2 to M1 phenotypes in the tumor microenvironment, Biomaterials, 112 (2017) 153-163.

[17] J. Conde, C. Bao, Y. Tan, D. Cui, E.R. Edelman, H.S. Azevedo, H.J. Byrne, N. Artzi, F. Tian, Dual targeted immunotherapy via in vivo delivery of biohybrid RNAi-peptide nanoparticles to tumour-associated macrophages and cancer cells, Adv Funct Mater, 25 (2015) 4183-4194.

[18] Y. Qian, S. Qiao, Y. Dai, G. Xu, B. Dai, L. Lu, X. Yu, Q. Luo, Z. Zhang, Molecular-Targeted Immunotherapeutic Strategy for Melanoma via Dual-Targeting Nanoparticles Delivering Small Interfering RNA to Tumor-Associated Macrophages, ACS Nano, 11 (2017) 9536-9549.

[19] M.F. Cuccarese, J.M. Dubach, C. Pfirschke, C. Engblom, C. Garris, M.A. Miller, M.J. Pittet, R. Weissleder, Heterogeneity of macrophage infiltration and therapeutic response in lung carcinoma revealed by 3D organ imaging, Nat Commun, 8 (2017) 14293.

[20] J.L. Guerriero, A. Sotayo, H.E. Ponichtera, J.A. Castrillon, A.L. Pourzia, S. Schad, S.F. Johnson, R.D. Carrasco, S. Lazo, R.T. Bronson, S.P. Davis, M. Lobera, M.A. Nolan, A. Letai, Class IIa HDAC inhibition reduces breast tumours and metastases through anti-tumour macrophages, Nature, 543 (2017) 428-432.

[21] F.T. Andón, E. Digifico, A. Maeda, M. Erreni, A. Mantovani, M.J. Alonso, P. Allavena, Targeting tumor associated macrophages: The new challenge for nanomedicine, Semin Immunol, 34 (2017) 103-113.

[22] S.M. Pyonteck, L. Akkari, A.J. Schuhmacher, R.L. Bowman, L. Sevenich, D.F. Quail, O.C. Olson, M.L. Quick, J.T. Huse, V. Teijeiro, M. Setty, C.S. Leslie, Y. Oei, A. Pedraza, J. Zhang, C.W. Brennan, J.C. Sutton, E.C. Holland, D. Daniel, J.A. Joyce, CSF-1R inhibition alters macrophage polarization and blocks glioma progression, Nat Med, 19 (2013) 1264-1272.

[23] A. Ramesh, S. Kumar, D. Nandi, A. Kulkarni, CSF1R- and SHP2-Inhibitor-Loaded Nanoparticles Enhance Cytotoxic Activity and Phagocytosis in Tumor-Associated Macrophages, Adv Mater, 31 (2019) e1904364.

[24] N. Vinod, D. Hwang, S.H. Azam, A.E.D. Van Swearingen, E. Wayne, S.C. Fussell, M. Sokolsky-Papkov, C.V. Pecot, A.V. Kabanov, High-capacity poly(2-oxazoline) formulation of TLR 7/8 agonist extends survival in a chemo-insensitive metastatic model of lung adenocarcinoma, Sci Adv, 6 (2020) eaba5542.

[25] H. Chi, C. Li, F.S. Zhao, L. Zhang, T.B. Ng, G. Jin, O. Sha, Anti-tumor Activity of Toll-Like Receptor 7 Agonists, Front Pharmacol, 8 (2017) 304.

[26] C.B. Rodell, S.P. Arlauckas, M.F. Cuccarese, C.S. Garris, R. Li, M.S. Ahmed, R.H. Kohler, M.J. Pittet, R. Weissleder, TLR7/8-agonist loaded nanoparticles promote the polarization of tumour-associated macrophages to enhance cancer immunotherapy, Nat Biomed Eng, 2 (2018) 578-588.

[27] A.L. Engel, G.E. Holt, H. Lu, The pharmacokinetics of Toll-like receptor agonists and the impact on the immune system, Expert Rev Clin Pharmacol, 4 (2011) 275-289.

[28] R.P. Tobin, K.R. Jordan, W.A. Robinson, D. Davis, V.F. Borges, R. Gonzalez, K.D. Lewis, M.D. McCarter, Targeting myeloid-derived suppressor cells using all-trans retinoic acid in melanoma patients treated with Ipilimumab, Int Immunopharmacol, 63 (2018) 282-291.

[29] Y. Nefedova, M. Fishman, S. Sherman, X. Wang, A.A. Beg, D.I. Gabrilovich, Mechanism of all-trans retinoic acid effect on tumor-associated myeloid-derived suppressor cells, Cancer Res, 67 (2007) 11021-11028.

[30] D.E. Tsai, S.M. Luger, A. Kemner, C. Swider, A. Goradia, E. Tomczak, D. DiPatri, A. Bagg, P. Nowell, A.W. Loren, A. Perl, S. Schuster, J.E. Thompson, D. Porter, C. Andreadis, E.A. Stadtmauer, S. Goldsteini, R. Ghalie, M. Carroll, Evidence of myeloid differentiation in non-M3 acute myeloid leukemia treated with the retinoid X receptor agonist bexarotene, Cancer Biol Ther, 6 (2007) 18-21.

[31] K. Tanita, T. Fujimura, Y. Sato, C. Lyu, Y. Kambayashi, D. Ogata, S. Fukushima, A. Miyashita, H. Nakajima, M. Nakamura, A. Morita, S. Aiba, Bexarotene Reduces Production of CCL22 From Tumor-Associated Macrophages in Cutaneous T-Cell Lymphoma, Front Oncol, 9 (2019) 907.

[32] C.F. Chang, J. Massey, A. Osherov, L.H. Angenendt da Costa, L.H. Sansing, Bexarotene Enhances Macrophage Erythrophagocytosis and Hematoma Clearance in Experimental Intracerebral Hemorrhage, Stroke, 51 (2020) 612-618.

[33] L. Li, Y. Liu, J. Wang, L. Chen, W. Zhang, X. Yan, Preparation, in vitro and in vivo evaluation of bexarotene nanocrystals with surface modification by folate-chitosan conjugates, Drug Deliv, 23 (2016) 79-87.

[34] J. Sun, Y. Chen, J. Xu, X. Song, Z. Wan, Y. Du, W. Ma, X. Li, L. Zhang, S. Li, High Loading of Hydrophobic and Hydrophilic Agents via Small Immunostimulatory Carrier for Enhanced Tumor Penetration and Combinational Therapy, Theranostics, 10 (2020) 1136-1150.

[35] T.H. Tran, R. Rastogi, J. Shelke, M.M. Amiji, Modulation of Macrophage Functional Polarity towards Anti-Inflammatory Phenotype with Plasmid DNA Delivery in CD44 Targeting Hyaluronic Acid Nanoparticles, Sci Rep, 5 (2015) 16632.

[36] J.M. Rios de la Rosa, A. Tirella, A. Gennari, I.J. Stratford, N. Tirelli, The CD44-Mediated Uptake of Hyaluronic Acid-Based Carriers in Macrophages, Adv Health Mater, 6 (2017).

[37] M.A. Sallam, S. Prakash, V. Krishnan, K. Todorova, A. Mandinova, S. Mitragotri, Hyaluronic Acid Conjugates of Vorinostat and Bexarotene for Treatment of Cutaneous Malignancies, Advanced Therapeutics, n/a 2000116.

[38] M.A. Evans, C.W. Shields IV, V. Krishnan, L.L.-W. Wang, Z. Zhao, A. Ukidve, M. Lewandowski, Y. Gao, S. Mitragotri, Macrophage-Mediated Delivery of Hypoxia-Activated Prodrug Nanoparticles, Advanced Therapeutics, 3 (2020) 1900162.

[39] I. Mottas, A. Bekdemir, A. Cereghetti, L. Spagnuolo, Y.S. Yang, M. Müller, D.J. Irvine, F. Stellacci, C. Bourquin, Amphiphilic nanoparticle delivery enhances the anticancer efficacy of a TLR7 ligand via local immune activation, Biomaterials 190-191 (2019) 111-120.

[40] H. Shinchi, B. Crain, S. Yao, M. Chan, S.S. Zhang, A. Ahmadiiveli, Y. Suda, T. Hayashi, H.B. Cottam, D.A. Carson, Enhancement of the Immunostimulatory Activity of a TLR7 Ligand by Conjugation to Polysaccharides, Bioconjug Chem, 26 (2015) 1713-1723.

[41] E.L. Smits, P. Ponsaerts, Z.N. Berneman, V.F. Van Tendeloo, The use of TLR7 and TLR8 ligands for the enhancement of cancer immunotherapy, Oncologist, 13 (2008) 859-875.

[42] J. Klarquist, K. Tobin, P. Farhangi Oskuei, S.W. Henning, M.F. Fernandez, E.R. Dellacecca, F.C. Navarro, J.M. Eby, S. Chatterjee, S. Mehrotra, J.I. Clark, I.C. Le Poole, Ccl22 Diverts T Regulatory Cells and Controls the Growth of Melanoma, Cancer Res, 76 (2016) 6230-6240.

[43] L. Li, X. Liu, K.L. Sanders, J.L. Edwards, J. Ye, F. Si, A. Gao, L. Huang, E.C. Hsueh, D.A. Ford, D.F. Hoft, G. Peng, TLR8-Mediated Metabolic Control of Human Treg Function: A Mechanistic Target for Cancer Immunotherapy, Cell Metab, 29 (2019) 103-123.e105.

[44] C. Hotz, C. Bourquin, Systemic cancer immunotherapy with Toll-like receptor 7 agonists: Timing is everything, Oncoimmunology, 1 (2012) 227-228.

[45] C. Bourquin, C. Hotz, D. Noerenberg, A. Voelkl, S. Heidegger, L.C. Roetzer, B. Storch, N. Sandholzer, C. Wurzenberger, D. Anz, S. Endres, Systemic cancer therapy with a small molecule agonist of toll-like receptor 7 can be improved by circumventing TLR tolerance, Cancer Res, 71 (2011) 5123-5133.

[46] E. Orsini, A. Guarini, S. Chiaretti, F.R. Mauro, R. Foa, The circulating dendritic cell compartment in patients with chronic lymphocytic leukemia is severely defective and unable to stimulate an effective T-cell response, Cancer Res, 63 (2003) 4497-4506.

[47] P. Tripathi, P. Tripathi, L. Kashyap, V. Singh, The role of nitric oxide in inflammatory reactions, FEMS Immunology & Medical Microbiology, 51 (2007) 443-452.

[48] T. Wang, H. Liu, G. Lian, S.Y. Zhang, X. Wang, C. Jiang, HIF1α-Induced Glycolysis Metabolism Is Essential to the Activation of Inflammatory Macrophages, Mediators Inflamm, 2017 (2017) 9029327.

[49] E.R. Watts, S.R. Walmsley, Inflammation and Hypoxia: HIF and PHD Isoform Selectivity, Trends Mol Med, 25 (2019) 33-46.

[50] C.W.t. Shields, M.A. Evans, L.L. Wang, N. Baugh, S. Iyer, D. Wu, Z. Zhao, A. Pusuluri, A. Ukidve, D.C. Pan, S. Mitragotri, Cellular backpacks for macrophage immunotherapy, Sci Adv, 6 (2020) eaaz6579.

[51] A. Kulkarni, V. Chandrasekar, S.K. Natarajan, A. Ramesh, P. Pandey, J. Nirgud, H. Bhatnagar, D. Ashok, A.K. Ajay, S. Sengupta, A designer self-assembled supramolecule amplifies macrophage immune responses against aggressive cancer, Nat Biomed Eng, 2 (2018) 589-599.

[52] E. Markovsky, H. Baabur-Cohen, R. Satchi-Fainaro, Anticancer polymeric nanomedicine bearing synergistic drug combination is superior to a mixture of individually-conjugated drugs, J Control Release, 187 (2014) 145-157.

[53] T. Lammers, V. Subr, K. Ulbrich, P. Peschke, P.E. Huber, W.E. Hennink, G. Storm, Simultaneous delivery of doxorubicin and gemcitabine to tumors in vivo using prototypic polymeric drug carriers, Biomaterials, 30 (2009) 3466-3475.

[54] S. Luo, Y. Gu, Y. Zhang, P. Guo, J.F. Mukerabigwi, M. Liu, S. Lei, Y. Cao, H. He, X. Huang, Precise Ratiometric Control of Dual Drugs through a Single Macromolecule for Combination Therapy, Mol Pharm, 12 (2015) 2318-2327.

[55] A. Ukidve, Z. Zhao, A. Fehnel, V. Krishnan, D.C. Pan, Y. Cao, A. Mandal, V. Muzykantov, S. Mitragotri, Erythrocyte-driven immunization via biomimicry of their natural antigen-presenting function, Proc Natl Acad Sci U S A, 117 (2020) 17727-17736.

[56] K.M. Camacho, S. Kumar, S. Menegatti, D.R. Vogus, A.C. Anselmo, S. Mitragotri, Synergistic antitumor activity of camptothecin-doxorubicin combinations and their conjugates with hyaluronic acid, J Control Release, 210 (2015) 198-207.

[57] D.R. Vogus, M.A. Evans, A. Pusuluri, A. Barajas, M. Zhang, V. Krishnan, M. Nowak, S. Menegatti, M.E. Helgeson, T.M. Squires, S. Mitragotri, A hyaluronic acid conjugate engineered to synergistically and sequentially deliver gemcitabine and doxorubicin to treat triple negative breast cancer, J Control Release, 267 (2017) 191-202.

[58] D. Vogus, V. Krishnan, S. Mitragotri, A review on engineering polymer drug conjugates to improve combination chemotherapy, Current Opinion in Colloid & Interface Science, 31 (2017).

Credit Statement

M.S. and S.M. designed the research. M.S., C.W.S, S.P., J.K., D.P. performed the experiments,

M.S., C.W.S. and S.M. analyzed the data. M.S. and S.M. wrote the paper with revisions from all

authors. S.M. conceived the project.

Graphical abstract

Highlights

- Re-education of TAMs from M2 to M1 phenotype is an attractive approach for melanoma.
- Resiquimod and bexarotene promote macrophage polarization to antitumoral phenotype.
- Clinical translation of both drugs is hindered by poor pharmacokinetics.
- Conjugation of resiquimod and bexarotene to HA allowed their coadministration.
- The dual conjugate inhibited melanoma growth better than the single drug conjugates.